Fuel Performance Calculations for FeCrAl Cladding in BWRs

Nathan M. George[1], Ryan T. Sweet[1], G. Ivan Maldonado[1], Brian D. Wirth[1], Jeffrey J. Powers[2], Andrew Worrall[2]
[1] *Department of Nuclear Engineering, University of Tennessee, Knoxville, TN 37996*
[2] *Reactor and Nuclear Systems Division, Oak Ridge National Laboratory, Oak Ridge, TN 37831*

INTRODUCTION

The outcome of a severe accident scenario in a light water reactor is largely dominated by the types and availability of safety systems and the sequence of events. In loss-of-coolant scenarios, decay heat, coupled with poor heat transfer to steam, drives up the core temperature. Physical and chemical degradation phenomena occur at temperatures above approximately 800°C, at which point the fuel rod bursts [1]. As the core temperature increases, detrimental steam oxidation of core constituents exacerbates core degradation processes, compromising core cooling and depositing large amounts of enthalpy from oxidation and radioactive decay [2]. Given these factors, efforts are underway to find alternate fuel-cladding concepts that exhibit slower oxidation kinetics in high-temperature steam environments compared with zirconium alloys (Zircaloy) [3–5].

This study expands upon previous neutronics analyses of the reactivity impact of alternate cladding concepts in boiling water reactor (BWR) cores [6,7] and directs focus toward contrasting fuel performance characteristics of FeCrAl cladding against those of traditional Zircaloy. Using neutronics results from a modern version of the 3D nodal simulator NESTLE [8], linear power histories were generated and supplied to the BISON-CASL code [9,10] for fuel performance evaluations. BISON-CASL (formerly Peregrine) expands on material libraries implemented in the BISON fuel performance code [11] and the MOOSE framework [12] by providing proprietary material data. By creating material libraries for Zircaloy and FeCrAl cladding, the thermomechanical behavior of the fuel rod (e.g., strains, centerline fuel temperature, and time to gap closure) were investigated and contrasted.

METHODOLOGY

Coupling BISON-CASL and NESTLE

Power histories (maximum linear heat generation rates) for a representative BWR cycle depletion were calculated with the NESTLE full-core simulator and were fitted axially to a two-dimensional RZ fuel rod model created with BISON-CASL. By combining full-core and lattice physics analyses, the most limiting fuel rod at each available time step of the depletion cycle was selected for evaluation with the fuel performance code. By using an equilibrium cycle, future cycle assemblies were selected on the basis of end-of-cycle burnup of the previous cycle's limiting assembly. This process was repeated to produce maximum linear heat generation rates for three 18-month cycles.

Nodal temperatures were transferred from the thermal hydraulic results of NESTLE for implementation in the fuel performance model. Throughout the depletion cycle, fluctuations in the bulk coolant temperature were captured and used for boundary condition settings to establish the fuel rod temperature profile in BISON-CASL. Lastly, the peak fast fluxes were gathered from both the Zircaloy and FeCrAl lattice physics calculations within an energy range between 1 and 10 MeV.

BISON-CASL Simulations of FeCrAl and Zircaloy

A 2D BISON-CASL simulation input and a geometric fuel rod model (shown in Figure 1) were developed using results from NESTLE. The fuel in the geometric model is simplified by using a single smeared fuel pellet spanning the length of the rod. Red cells indicate the UO_2 fuel region; blue represents the cladding.

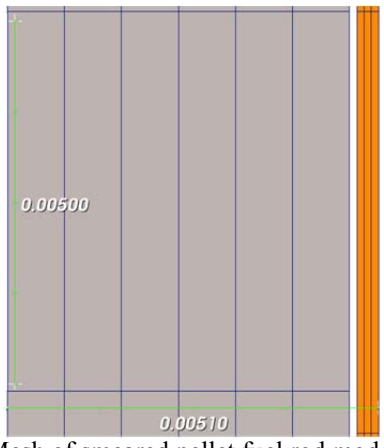

Figure 1: Mesh of smeared pellet fuel rod model with 300 μm cladding

BISON-CASL simulations utilize the provided power history and axial peaking factors of the fuel rod to determine the power produced in the fuel rod at a specific time. This, in turn, allows the temperature to be calculated along with other dependent material properties through the lifetime of the fuel. To simulate the UO_2 fuel, these properties were determined using previously developed models including Nuclear Fuel Industry Research (NFIR) temperature- and burnup-dependent thermal properties; temperature-dependent mechanical properties; fuel swelling, densification, and relocation; thermal and irradiation creep; and fission gas release. The gap and plenum regions of the fuel are modeled with heat transfer from the fuel to the clad and an applied pressure on the inside of the clad and outside of the fuel, which is based on the composition and quantity of fission gas released into the regions as well as the volume the gas occupies. Models for the Zircaloy cladding include temperature-dependent thermal and mechanical properties, thermal and irradiation creep, and irradiation growth.

In order for BISON-CASL to simulate different materials, models of the materials must first be created. The models contain data regarding the chemical, mechanical, and thermal properties of the material and are as complex or simple as the available data. Material models for FeCrAl were based on datasheets for several alloys [13], with various material properties taken and fitted to curves based on their dependencies. These models are based on available thermophysical, mechanical, and irradiation properties and include thermal conductivity, specific heat, elastic modulus, density, thermal strain, and irradiation swelling, among others.

Three BISON-CASL simulations were performed to analyze fuel performance differences between FeCrAl- and Zircaloy-cladded fuel elements during normal reactor operation. The simulations were designed to demonstrate the irradiation swelling effect in FeCrAl cladding and in Zircaloy cladding in order to compare the two cladding types. The axial and radial displacements are useful for determining if the cladding will expand or swell too much during operation. If the cladding elongates excessively in the axial direction, the fuel risks bowing or deforming due to size constraints, and if the cladding radius increases too much, the fuel risks increased contact with the fuel assembly spacer grid. The fuel rod geometries were generated based on the rough specifications of the representative BWR core and the expected requirements of using a FeCrAl alloy (shown in Table I).

Table I: Fuel performance geometry specifications

Cladding Type	Fuel Radius (μm)	Gap Thickness (μm)	Cladding Thickness (μm)	Fuel Length (m)	Cladding Length (m)	Enrichment (% U-235)
Zircaloy	4400	100	600	3.66	4.08	4.11
FeCrAl	4700		300			4.68

For the preliminary comparison of the FeCrAl and Zircaloy simulations, the peak fuel centerline temperature, axial and radial elongation, and gap closure time were compared. Determining the fuel centerline temperature is useful in fuel performance to estimate how close the UO_2 fuel is to its melting temperature (~3100 K). As the fuel reaches the melting temperature, it begins to deform and compromise the fuel geometry. The onset of gap closure marks the onset of phenomena including increased heat transfer from the fuel to the cladding by eliminating the gap. This, in turn, increases tensile azimuthal stresses in the cladding as the fuel adds additional forces to the inner surface of the cladding.

RESULTS

Thermomechanical fuel performance calculations were performed using BISON-CASL. Unfortunately, once contact of the fuel pellet and cladding began, the number of constraints applied to the finite element mesh increased, degrading the solver performance and slowing the simulation. Changes to user-specified spatial mesh, time steps, or modeling parameters chosen for the BISON-CASL simulations could improve some of these issues during pellet-cladding contact. The results presented herein are shown up to approximately 700 EFPD, which represents about half of the life of a standard fuel rod. Figure 2 plots the peak fuel centerline temperature for FeCrAl with and without swelling. The FeCrAl cladding with swelling exhibits the highest temperature at the end of the depletion sequence. This should be expected compared to Zircaloy because the fuel radius of the FeCrAl models is larger, and the thermal conductivity of UO_2 is low. The temperature of the FeCrAl cladding with swelling should also be larger than that without swelling because the cladding slowly increases in size as it swells, thus opening the fuel-cladding gap and degrading the heat transfer from the fuel to the cladding.

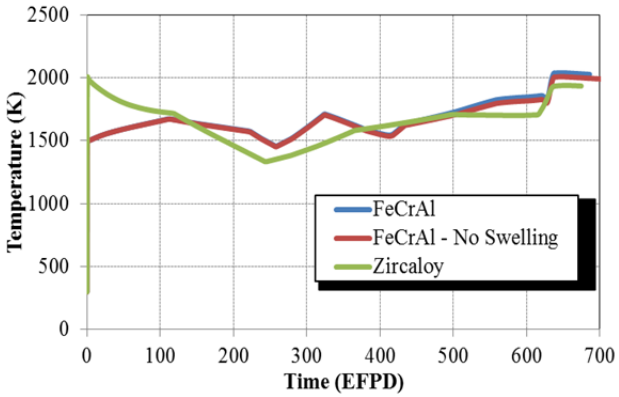

Figure 2: Peak centerline temperature

In both cases (axial and radial, shown in Figure 3 and Figure 4), FeCrAl with swelling undergoes greater displacement than FeCrAl without swelling or Zircaloy. This is potentially due to the thickness of the FeCrAl cladding, which is half that of the Zircaloy cladding, generating greater stresses on the cladding. The FeCrAl with swelling should also have greater displacements than the alloy without swelling because of the presence of isotropic volumetric swelling. Excessive clad swelling in the axial and radial directions can lead to fuel rod bowing as well as increased fretting wear. Therefore, future work will need to analyze the mechanical implications of how additional swelling might affect reactor operation.

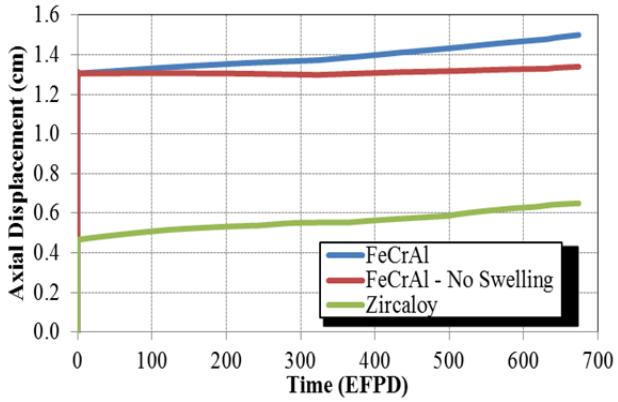

Figure 3: Axial displacement throughout depletion

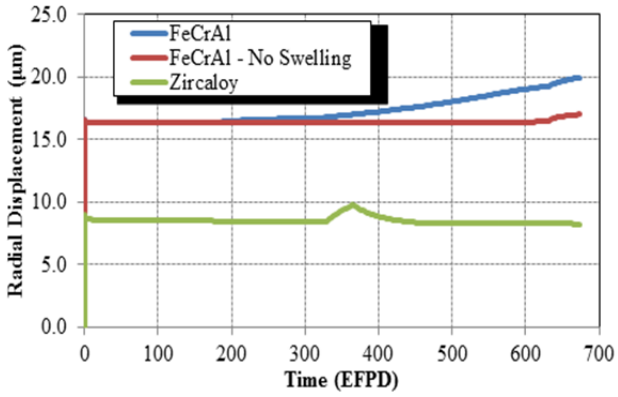

Figure 4: Radial displacement throughout depletion

Gap closure times were determined very roughly to be 697 EFPD for FeCrAl, 700 EFPD for FeCrAl without swelling, and 278 EFPD for the Zircaloy cladding. This demonstrates that the effect of swelling on gap closure is very small, but FeCrAl closes much later than Zircaloy due to its greater radial displacements. This is most likely an effect of the axial power profiles that are applied separately for each different type of cladding. The burnup distribution across the FeCrAl core is less than that for the Zircaloy core because the FeCrAl model contained a higher heavy metal loading, leading to lower linear heat rates and smaller expansion of the UO_2 pellet. If the power peaks in a single area, the fuel in that area will expand faster than in other areas; therefore, local gap closure will occur in that area much sooner than in the rest of the fuel rod.

CONCLUSIONS

Fuel performance analysis of FeCrAl-cladded fuel rods was performed with the BISON-CASL code. By linking the linear heat rate results from NESTLE, the limiting fuel rods from the FeCrAl and Zircaloy cores were compared. Due to the lower power history profile in the FeCrAl model, the expansion of the UO_2 pellet was minimized; thus, the gap closure time for FeCrAl occurred at 700 EFPD, whereas the closure for Zircaloy occurred at 278 EFPD. However, due to the larger overall fuel pellet radius in the FeCrAl model, the overall thermal conductivity in the fuel rod was decreased, thereby leading to slightly higher centerline temperatures. The fuel performance calculations also showed an increase in radial and axial expansion for FeCrAl.

ACKNOWLEDGMENT

The authors wish to thank Kurt Terrani of Oak Ridge National Laboratory for his helpful insight and contributions to this work. Portions of this work were supported by the US DOE Integrated University Program Graduate Fellowship program and US DOE Nuclear Energy University Programs funds. BISON-CASL simulations were performed using the Fission supercomputer of the High Performance Computing Center at the Idaho National Laboratory.

REFERENCES

1. Hofmann, P., *Current knowledge on core degradation phenomena, a review*. Journal of Nuclear Materials, 1999. **270**(1): p. 194–211.
2. Steinbrück, M., et al., *Synopsis and outcome of the QUENCH experimental program*. Nuclear Engineering and Design, 2010. **240**(7): p. 1714–1727.
3. Terrani, K.A., S.J. Zinkle, and L. L. Snead, *Advanced oxidation-resistant iron-based alloys for LWR fuel cladding*. Journal of Nuclear Materials, 2014. **448**: p. 420–435.
4. Pint, B.A., et al., *High temperature oxidation of fuel cladding candidate materials in steam-hydrogen environments*. Journal of Nuclear Materials, 2013. **440**: p. 420–427.
5. Moalem, M., and D.R. Olander, *Oxidation of Zircaloy by steam*. Journal of Nuclear Materials, 1991. **182**: p. 170–194.
6. George, N.M., et al., *Development of a Full-Core Reactivity Equivalence for FeCrAl Enhanced*

Accident Tolerant Fuel in BWRs. Proc. Advances in Nuclear Fuel Management V (ANFM V). Hilton Head, SC, March 29 – April 1, 2015.
7. George, N.M., et al., *Validation of a Full-Core Reactivity Equivalence for FeCrAl Enhanced Accident Tolerant Fuel in BWRs*. Proc. Advances in Nuclear Fuel Management V (ANFM V). Hilton Head, SC, March 29 – April 1, 2015.
8. Luciano, N.P., et al., *The NESTLE 3D Nodal Core Simulator: Modern Reactor Models*, Proc. MC2015 Joint International Conference on Mathematics and Computation (M&C). Nashville, TN, April 19–23, 2015.
9. Montgomery, R., et al., *Peregrine: Advanced Modeling of Pellet-Cladding Interaction (PCI) Failure in LWRs*, Proc. TopFuel 2012 Reactor Fuel Performance Conference. Manchester, United Kingdom, September 2–6, 2012. European Nuclear Society, (2012).
10. Montgomery, R.O., et al., *Peregrine: Validation and Benchmark Evaluation of Integrated Fuel Performance Modeling Using Test Reactor Data and Falcon*. CASL Milestone Report L1.CASL.P7.02, Oak Ridge, TN, June 2013.
11. Williamson, R., et al., *Multidimensional multiphysics simulation of nuclear fuel behavior*. Journal of Nuclear Materials, 2012. **423**: 149–163.
12. Gaston, D., et al., *MOOSE: A parallel computational framework for coupled systems of nonlinear equations*. Nuclear Engineering and Design, 2009. **239**(10): p. 1768-1778.
13. Kanthal, A., *APMT Tube Material Datasheet*. AB Sandvik group, Sandviken, Sweden.